

IFUSP/P 707  
B.I.F. - USP

UNIVERSIDADE DE SÃO PAULO

# PUBLICAÇÕES

INSTITUTO DE FÍSICA  
CAIXA POSTAL 20516  
01498 - SÃO PAULO - SP  
BRASIL

IFUSP/P-707

Contributed Papers

III LATIN-AMERICAN WORKSHOP IN PLASMA PHYSICS  
(Santiago, 1988)

by the

TBR-1 Team

Instituto de Física, Universidade de São Paulo

26 MAI 1988



Maio/1988

DESTRUCTION OF MAGNETIC SURFACES IN LARGE ASPECT-RATIO TOKAMAKS

M.V.A.P. Heller, I.L. Caldas

Instituto de Física, USP  
C.P. 20.516, 01498 - São Paulo, SP, Brazil

**Abstract:** Magnetic surface break-up in tokamaks caused by overlapping of magnetic islands, created by helical windings and plasma oscillations, is evaluated integrating numerically the differential equation for the magnetic field lines.

The objective of this work is to investigate the destruction of magnetic surfaces caused by the superposition of different helical resonances. To do that the differential equation for the magnetic field lines  $\vec{B} \times d\vec{x} = 0$  is numerically integrated. It is considered a linear superposition of the equilibrium field with the resonant helical perturbations created by helical windings and by plasma oscillations. Resonances due to the toroidal corrections were also considered. Typical parameters of the Brazilian tokamak TBR-1 were used in the numerical applications.

A plasma confined in a large aspect-ratio tokamak is represented by a periodical cylinder with length  $2\pi R$  and radius  $a$ . The MHD equilibrium is determined by the poloidal  $B_{\theta 0}$  and the toroidal  $B_{z 0}$  magnetic field components. The unperturbed magnetic surfaces are characterized by the safety factor  $q = (rB_{z 0}) / (RB_{\theta 0})$ .

A helical resonance of the type  $f(r)\cos(m\theta - nz/R)$  creates  $m$  magnetic islands with width  $\Delta\alpha f^{1/2}$  around the surface with  $q=m/n$ .

Magnetic oscillations observed in tokamaks are related to helical current perturbations on the unperturbed rational surface with  $q=m/n$ <sup>(1)</sup>. These currents are distributed poloidally and toroidally according to the relative phases of the detected Mirnov oscillations. Their amplitudes depend on the measured amplitude of the plasma oscillation  $\delta B_{\theta m,n}$ . In this case  $\Delta\alpha(\delta B_{\theta m,n})^{1/2}$ .

Electrical currents  $I$  flowing in  $m$  pairs of helical windings, wound on a large aspect-ratio tokamak<sup>(1)</sup>, are also considered. For currents flowing in opposite directions in adjacent windings  $\Delta\alpha(I)^{1/2}$ .

When a single helical perturbation  $(m, n)$  is superimposed upon an equilibrium with toroidal symmetry both symmetries are broken, and the magnetic

surfaces may disappear. For a small helical perturbation the major effect, on a large aspect-ratio tokamak, is the appearance of  $m\pm 1$  satellite islands (with width  $\Delta\alpha f^{1/4}$ ) on the surfaces with  $q=(m\pm 1)/n$ <sup>(2)</sup>. These islands have been taken into account by multiplying the constant  $B_{z 0}$  by the factor  $(1+r\cos\theta/R)^{-1}$  in the field line equation.

Magnetic surfaces break-up occurs due to the destruction of the system symmetry. As a symmetry breaking due to magnetic islands with different helicities grows, magnetic surfaces are destroyed. The degree of chaotic distribution of the magnetic lines outside the remaining magnetic surfaces depend upon the amplitudes  $I$  and  $\delta B_{\theta}$ . This dependence can be indicated by the stochasticity parameter  $S$  defined as

$$S = \frac{\Delta_{m,n} + \Delta_{m',n'}}{2(r_{m,n} - r_{m',n'})} ; q(r_{m,n}) = m/n$$

The differential equation for the magnetic field lines have been integrated numerically for various perturbation strengths. Fig. 1 shows the intersections of the magnetic field line trajectories with a poloidal plane  $z=0$  for an equilibrium with  $q(a) = 5$  and  $q(0) = 1$  perturbed by a  $m=2/n=1$  tearing mode with  $\delta B_{\theta}/B_{\theta 0} = 0,5\%$  and a  $3/1$  helical current of  $100A(S=1.05)$  and  $300A(S=1.34)$ . For the same equilibrium, it has also been considered the surfaces destruction due to the superposition of the islands created by a  $3/1$  helical current with its satellite islands.

The fractions  $\alpha(S)$  of intersections in the Poincaré map outside an area delimited by two circles including the intersections of the considered rational surfaces, were computed and indicated in the Figs. 2 and 4 for the mentioned cases. The flux  $F(S)$  related to a chaotic line going through the cylindrical surfaces associated to that area<sup>(3)</sup> were also computed and indicated in the Figs. 3 and 5 for these cases.

The level of the fluctuations  $\sigma_{\alpha}$  in the computed  $\alpha$  and  $F$  values was evaluated by considering several different starting points on the Poincaré map. As it is shown in Fig. 6,  $\sigma$  increases with  $S$  and saturates for  $S \geq 1.1$ . This might be considered as a realistic criterium to characterize the predominance of a chaotic zone between the considered rational sur-

faces. This situation seems to be responsible for the beginning of minor disruptions observed during the TBR-1 tokamak discharges<sup>(4)</sup>.

Acknowledgements: The authors are grateful to Dr. M. Brusati (JET) for useful discussions.

References

- (1) A.S. Fernandes, M.V.A.P. Heller, I.L. Caldas, Plasma Phys. Controlled Fusion, to be published.
- (2) M.Y. Kucinski, I.L. Caldas, Zeit.Naturforschung,

42a, 1124 (1987).

- (3) P.H. Rebut, M. Brusati, M. Hugon, P.P. Lallia, Proc. 11<sup>th</sup> Int. Conf. on Plasma Phys. and Thermonuclear Fusion (Kyoto, 1986), II, 187, Vienna, 1987.
- (4) A. Vannucci, I.L. Caldas, I.C. Nascimento, M.V. A.P. Heller, In these Proceedings.

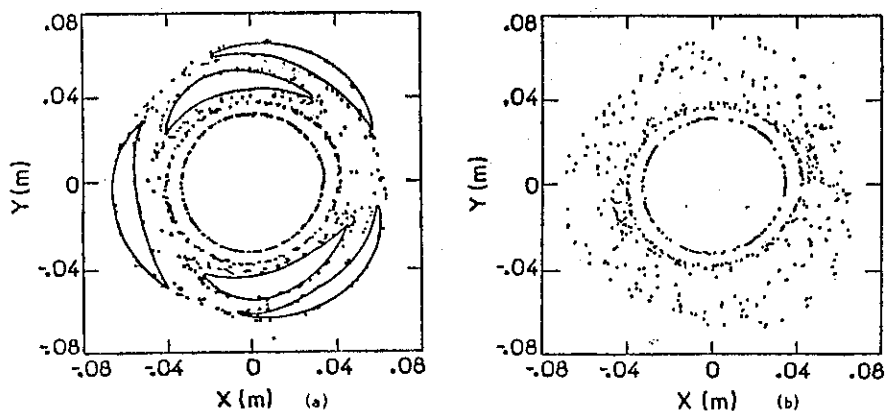


Fig. 1 - Intersections of magnetic field lines with a poloidal surface for  $q(a) = 5, q(0) = 1, \delta B_{\theta}(2/1) / B_{0\theta} = 0.52, I(3/1) = 100A(a)$  and  $300A(b)$ .

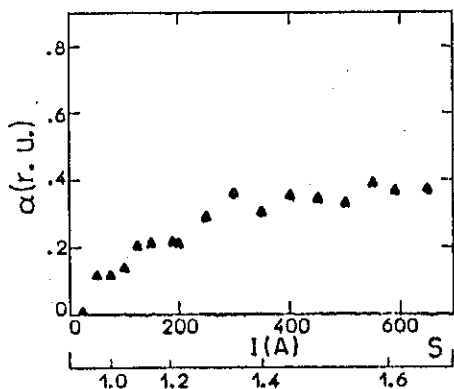


Fig. 2 - Variation of  $\alpha$  as a function of  $I$  and  $S$  for the case specified in the Fig. 1.

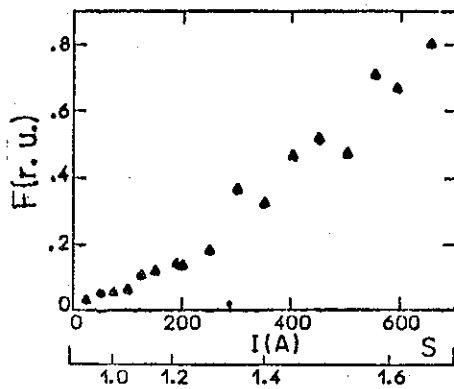


Fig. 3 - Variation of  $F$  as a function of  $I$  and  $S$  for the case specified in the Fig. 1.

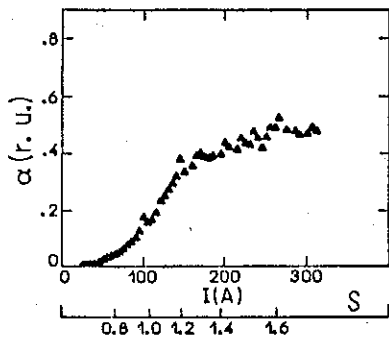


Fig. 4 - Variation of  $\alpha$  as a function of  $3/1$  helical current  $I$  and  $S$  for  $q(a) = 5$  and  $q(0) = 1.5$ . Satellite resonances were considered.

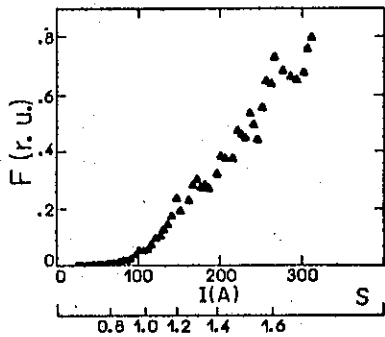


Fig. 5 - Variation of  $F$  as a function of  $3/1$  helical current  $I$  and  $S$  for  $q(a) = 5$  and  $q(0) = 1$ . Satellite resonances were considered.

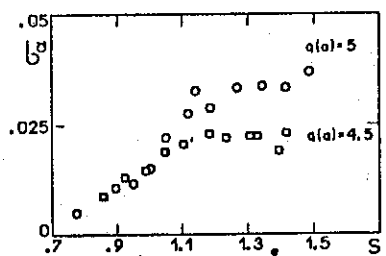


Fig. 6 - Standard deviation  $\sigma$  of the distribution of the computed values of  $\alpha$  as a function of  $S$ , for the case considered in Figs. 4 and 5, for two different values of  $q(a)$ .

A. Vannucci, I.L. Caldas, I.C. Nascimento, M.V.A.P. Heller

Instituto de Física da Universidade de São Paulo  
C.P. 20.516, 01498 - São Paulo, SP, Brazil

**Abstract:** Minor disruptions events were experimentally identified in the tokamak TBR-1 discharges. The main diagnostics used were a soft x-ray detection system and a set of 20 Mirnov coils. For well-formed confinements and the plasma column in the center of the vessel, these disruptions were associated to the destruction of the magnetic surfaces caused by the  $m/n=2/1$  and  $3/1$  magnetic islands.

The investigation of disruptive phenomena is usually done through the detection and analysis of perturbations in the macroscopic parameters of the plasma. Among them, the most relevant are the poloidal magnetic field oscillations and plasma temperature variations. Examining the behaviour of these fluctuations right before the instant at which the disruption begins one can experimentally evaluate the real processes that lead to a disruptive condition.

In the TBR-1 device ( $R_0=0.30\text{m}$ ,  $a=0.08\text{m}$ ,  $B_\phi=0.4\text{T}$  and  $6.0\text{A} \leq I_p \leq 12\text{kA}$ ) the soft x-ray emission from the plasma was detected by six surface barrier detectors, each one viewing a chord of the plasma column section through a polypropylene covered slit<sup>(1)</sup>. The poloidal magnetic field oscillations were measured by a set of twenty Mirnov coils, sixteen equally spaced in the poloidal direction and four in the toroidal direction<sup>(2)</sup>.

In the TBR-1 discharges, disruptive events characterized by a negative spike in the loop voltage, without the total loss of the confinement (so they could indeed be classified as minor disruptions), were observed in three different situations: i) whenever the adjustments of the equilibrium fields were not properly done, resulting in several minor disruptions all along the discharges; ii) when the magnetic islands start to grow and, due to plasma position displacements (due to the lack of a feedback controlling system for the plasma position), it hits the limiter and iii) when no one of these two cases happens and minor disruptions are still verified<sup>(1)</sup>.

In this paper we shall discuss only this last

situation, for which a typical discharge with  $q(a)=4.0$  is presented in Fig. 1. The signal output from the soft x-ray, the loop voltage and the pick-up coil systems (Figs. 1-c, 1-e and 1-d) show the exact instant at which the disruptions took place. Restricting ourselves to the last one of these disruptions, indicated in the figure by an arrow, the corresponding mhd activity was estimated to have a growth rate  $\gamma=6.6 \times 10^{-4}\text{s}^{-1}$ . Fourier analysing the Mirnov coils signals, it was also observed the  $m=3$  to be the dominant mode prior to this particular instability. The relative amplitude of the perturbed poloidal magnetic field was calculated, just before the appearance of the negative spike in the loop voltage, to be  $\bar{B}_\theta/B_\theta=1.2\%$ .

Taking the experimental perturbation amplitudes, corresponding to the  $m=2$  and  $m=3$  modes, the Poincaré maps for the field distribution were obtained by integrating the magnetic field line equations, determined in ref. 3. The results obtained are shown in Figs. 2-a and 2-b for two different times: 50 $\mu\text{s}$  before and in the instant of the negative spike appearance in the loop voltage, respectively.

Near the magnetic axis, where the field lines intersect a poloidal plane, a circle-like closed line is formed. Outwards, near the magnetic islands, the intersecting points do not describe a closed line anymore. They are displaced almost randomly and this effect is stronger for higher amplitude perturbations.

Comparing the pictures in Figs. 2-a and 2-b it is verified that the islands shrink and the chaotic region increases as the perturbation amplitude grows. This behaviour is consistent with the theory proposed by Finn<sup>(4)</sup> and others<sup>(5)</sup>. They associate the minor disruption with an interaction between magnetic islands due to the increase of the chaotic region around them. In the TBR-1 discharges the  $q=2$  and  $q=3$  magnetic islands would, therefore, interact in this way for a minor disruption occurrence.

References:

- (1) A. Vannucci, I.C. Nascimento, I.L. Caldas - "Disruptive Instabilities in the discharges of the TBR-1 small tokamak", to be published.
- (2) I.H. Tan, I.L. Caldas, I.C. Nascimento, R.P. da Silva, E.K. Sanada, R. Bruha - IEEE Trans. on Plasma Science PS-14 (1986) 279.
- (3) \* A.S. Fernandes, M.V.A.P. Heller, I.L. Caldas to be published in Plasma Phys. and Contr. Fusion.  
\* M.V.A.P. Heller, I.L. Caldas, in these proceedings.
- (4) J.M. Finn - Nucl. Fus. 15 (1975) 845.
- (5) A.B. Rechester, T.H. Stix - Phys. Rev. Lett. 36 (1976) 587.

Fig. 1 - Typical TBR-1 discharge with a sequence of minor disruptions observed in the soft x-ray(c), magnetic coil (d) and loop voltage (e) signals. The arrow indicates the disruptive event discussed in the text.

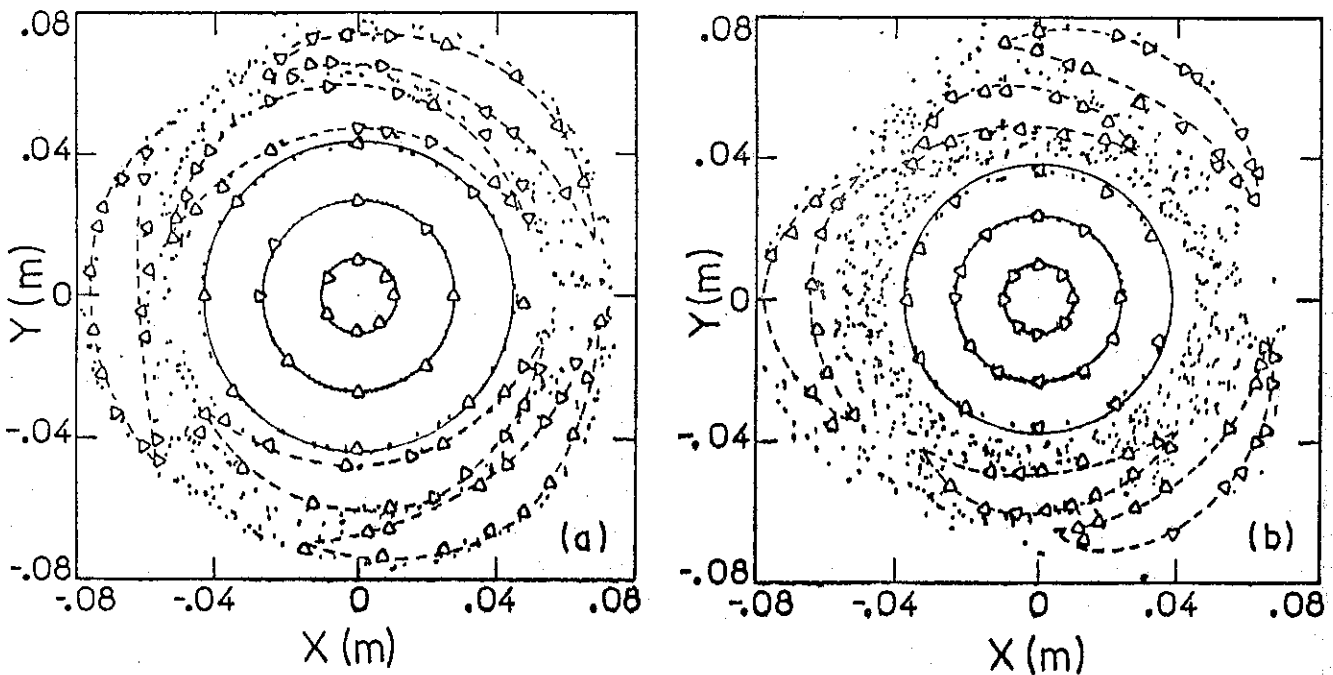
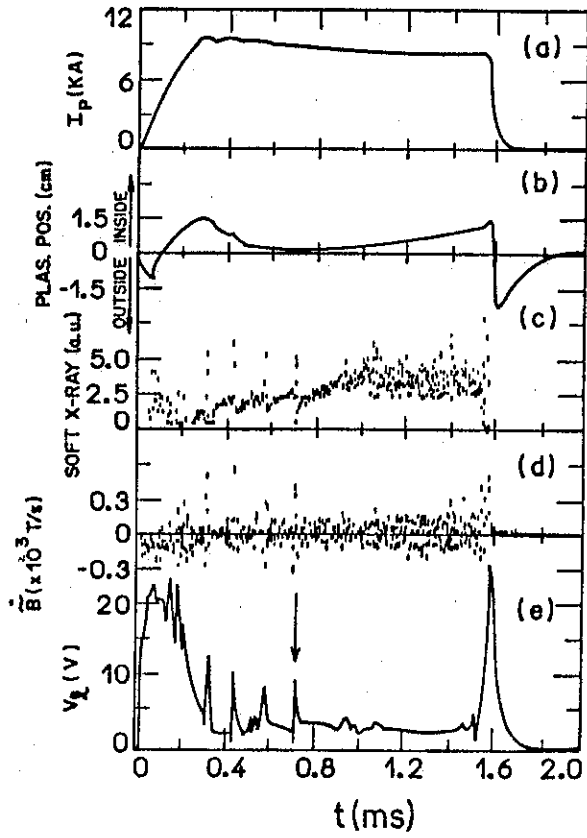


Fig. 2 - Intersections of magnetic field lines with a poloidal plane 50 $\mu$ s before (a) and in the instant (b) of the minor disruption indicated in the Fig. 1.

## MICROWAVE INTERFEROMETRY IN THE TBR-1 TOKAMAK

R.P. da Silva and J.C. Nascimento

Instituto de Física, Universidade de São Paulo  
C.P. 20.516, 01498 - São Paulo - SP, Brazil

### Introduction

In this work we describe the microwave interferometry system, built for the TBR-1 Tokamak<sup>[1]</sup>, and show results of electron density measurements in the central part of the plasma column. TBR-1 is a small tokamak designed at the Physics Institute of São Paulo University. Its main parameters are:  $R$  (major radius) = 30 cm,  $a$  (minor radius) = 8 cm,  $B_\phi$  (toroidal field) = 5 kG,  $I_p$  (Plasma Current) = 6 - 12 kA,  $n_e$  (electron density) =  $7 \times 10^{12} \text{ cm}^{-3}$  (centre),  $T_e$  (electron temperature) = 200 eV (centre).

The working principle for interferometry is the following: an electromagnetic wave is divided in two parts: one is used as reference and the other traverses the plasma. The two waves are mixed and the resulting signal analysed for phase shift.

### Theoretical Model

The theoretical model used in the data interpretation follows the theory of wave propagation in a cold plasma<sup>[2]</sup>. The wave is injected perpendicularly to the toroidal magnetic field ( $B_\phi$ ), with the wave electric field parallel to  $B_\phi$ . In this case the dispersion relation is

$$K_p = \frac{\omega}{c} \left[ 1 - \frac{n_e}{n_c} \right]^{1/2} \quad (1)$$

where  $K_p$  is the wave number in the plasma,  $\omega$  the wave frequency,  $n_e$  the electron density and  $n_c = (\epsilon_0 m_e \omega^2) / e^2$  the cut-off density. The effect of the collision was disregarded since  $\omega \gg \nu$ , the collision frequency (for TBR-1,  $\omega = 4 \times 10^{11} \text{ s}^{-1}$  and  $\nu \approx 8 \times 10^4 \text{ s}^{-1}$ ). Relation (1) shows that wave propagation properties depend only on electron density. If  $K_0 = \frac{\omega}{c}$  is the wave number in the vacuum, then the phase shift due to the plasma is given by:

$$\Delta\phi_p = \int_0^L (K_0 - K_p) dx \quad (2)$$

where the integration is performed along the length  $L$  in the plasma. If  $n_0 \ll n_c$ , (2) can be written in the form:

$$\Delta\phi_p = \frac{\pi}{\lambda} \frac{\bar{n}_e}{n_c} L \quad (3)$$

where  $\bar{n}_e$  is the average electron density in the plasma path. This expression shows that  $\bar{n}_e$  can be determined if the phase  $\Delta\phi_p$  is measured.

In our work a parabolic density profile was assumed,  $n_e(r) = n_0 [1 - (\frac{r}{a})^2]$ , where  $n_0$  is the center density and  $a$  the plasma radius. With this profile  $\bar{n} = 3 n_0 / 2$ . Using TBR-1 parameters follows the relation:

$$n_0 (\text{cm}^{-3}) = 7,2 \times 10^{11} \Delta\phi_p (\text{rd}) \quad (4)$$

### The TBR-1 Interferometer [3]

Fig. 1 shows a block diagram of the TBR-1 microwave interferometry system. The wave generator is a Klystron reflex (Variam VRE2101A18,  $f = 65 \text{ GHz}$ ,  $\lambda_0 = 4,6 \text{ mm}$  and  $P_{\text{max}} = 1 \text{ watt}$ ), that is coupled to an isolator. The wave is then divided in two parts by a 10 db directional coupler. One of them goes to the plasma and the other (the reference wave) pass through a variable attenuator (0-25 db) and a variable phase shifter (0-180°). The plasma and reference signal are mixed in a hybrid ring and applied to a square law detector. The injection and reception of the wave is made with two horn type antennas (gain = 25 dbi), located in the exterior part of the vessel. The wave passes through two quartz windows and a movable mechanical frame with 6 cm excursion allows measurements in different chords through the plasma.

An electronic system associated with the interferometer has been developed (Fig. 2). The system has three power supplies: for the resonator (200-3500V, 100mA); the reflector (0-1KV) and the heater (6,3x4A). The modulator has three different waveforms: sawtooth (0.1 to 100 kHz), square (0.1 to 100kHz) and sinusoidal (60 Hz), that can be used to modulate the Klystron frequency. The resonator power supply has adjustable overvoltage and over-current protection. The Klystron temperature is monitored and the power supply is switched off for temperatures higher than 90°. An amplifier with low-pass filters and adjustable gain, used for the detector signal, also has been built.

### Results[3]

The signal from the detector has the form:

$$V_S = V_0 + V_p \cos(\Delta\phi_p) \quad (5)$$

where  $V_0$  and  $V_p$  are constants. So, with the change of the density, there are oscillations in the detector output signal. In Fig. 3 the temporal profiles of the detector output signal and plasma current are shown. The plasma current has a maximum value 9kA and duration of 7ms. In this discharge hydrogen has been used with a filling pressure of  $1.3 \times 10^{-4}$  mbar. Between A and B, in Fig. 3, the pre-ionization of the plasma occurs, and between B and C the main plasma pulse. With the diode signal and the use of (5) and (4) relations the electron density time profile can be obtained. In Fig. 4 we see that, during the pre-ionization phase, the density reaches  $2.4 \times 10^{12} \text{ cm}^{-3}$  and then changes rapidly to  $7 \times 10^{12} \text{ cm}^{-3}$ , at the beginning of the main plasma pulse. From this point on the plasma current. We have seen that the maximum density changes with the filling pressure, and that the pre-ionization electron density has strong dependence on the toroidal field. Density and temperature measurements have also been made in the edge of plasma with electrostatic probes [4].

### Acknowledgements

The authors wish to thank Profs. I.L. Caldas and A.N. Fagundes for reading the manuscript.

### References

- [1] I.C. Nascimento, A.N. Fagundes, R.P. da Silva, R.M.O. Galvão, E. del Bosco, J.H. Vuolo, E.K. Sana and R. Dallaqua: Proceedings of the Spring College Fusion Energy, 1981 (International Centre for Theoretical Physics, Trieste, 1982), pg. 45.
- [2] M.A. Heald and C.B. Wharton - "Plasma diagnostic with microwaves". John Wiley and Sons Inc, New York, N.Y., 1965.
- [3] R.P. da Silva and I.C. Nascimento - "Microwave Interferometry in TBR-1". Internal Report 1988 (to be published).
- [4] R.P. da Silva, I.C. Nascimento, D.F. da Cruz Jr. and A. Hershovitch, Rev. Sci. Instrum. 57 (9), (1986) 2.205.

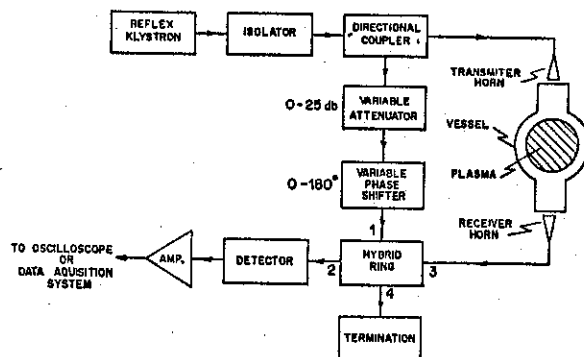


Fig. 1 - TBR-1 microwave interferometer.

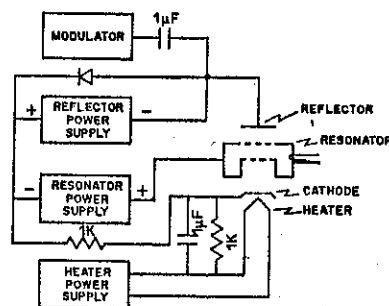


Fig. 2 - Klystron electronic system.

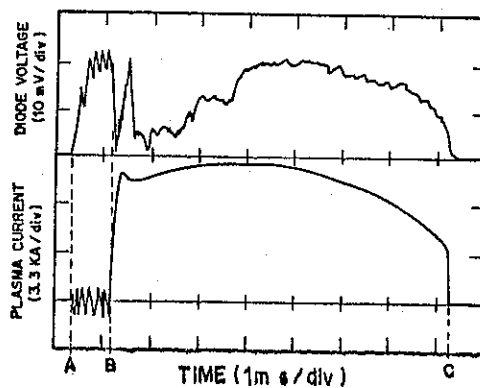


Fig. 3 - Diode Voltage and Plasma Current time profiles.

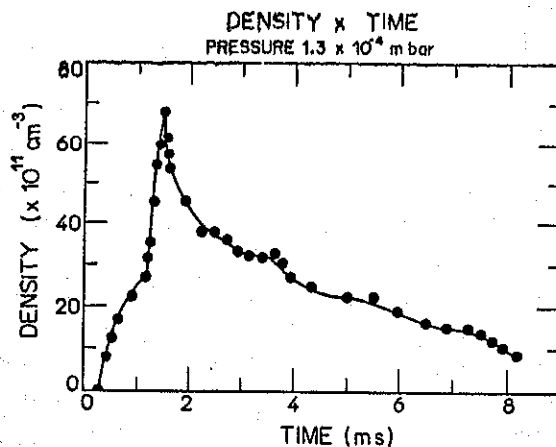


Fig. 4 - Density time profile.